

Perovskite phase stabilization in epitaxial $\text{Pb}(\text{Mg}_{1/3}\text{Nb}_{2/3})\text{O}_3\text{-PbTiO}_3$ films by deposition onto vicinal (001) SrTiO_3 substrates

S. D. Bu, M. K. Lee, and C. B. Eom^{a)}

Department of Materials Science and Engineering, University of Wisconsin-Madison, Madison, Wisconsin 53706

W. Tian and X. Q. Pan

Department of Materials Science and Engineering, The University of Michigan, Ann Arbor, Michigan 48109

S. K. Streiffer

Materials Science Division, Argonne National Laboratory, Argonne, Illinois 60439

J. J. Krajewski

Bell Laboratory, Lucent Technologies, Murray Hill, New Jersey 07974

(Received 11 June 2001; accepted for publication 6 September 2001)

We report the perovskite phase stabilization of $0.67\text{Pb}(\text{Mg}_{1/3}\text{Nb}_{2/3})\text{O}_3\text{-}0.33\text{PbTiO}_3$ (PMN-PT) epitaxial thin films by deposition onto miscut substrates. Films were grown on (001) SrTiO_3 substrates with miscut angles from 0 to 8 degrees toward the [100] direction using 90° off-axis magnetron sputtering. Films on high miscut substrates ($>4^\circ$) showed almost the pure perovskite phase in both x-ray diffraction and transmission electron microscopy image, and were nearly stoichiometric. In contrast, films on exact (001) SrTiO_3 contained a high volume fraction of pyrochlore phases with Pb deficiency. Atomic force microscopy reveals that films on 8° miscut substrates have a much smoother surface morphology than those on exact (001) SrTiO_3 . Cross-sectional transmission electron microscopy images reveal that the pyrochlore phases nucleate on top of the perovskite phase, and that the amount of the pyrochlore phases increase with film thickness. A film on an 8° miscut substrate exhibits a polarization hysteresis loop with a remnant polarization of $20 \mu\text{C}/\text{cm}^2$ at room temperature. © 2001 American Institute of Physics. [DOI: 10.1063/1.1414293]

Single crystal relaxor ferroelectrics, such as $\text{Pb}(\text{Mg}_{1/3}\text{Nb}_{2/3})\text{O}_3\text{-PbTiO}_3$ (PMN-PT) and $\text{Pb}(\text{Zn}_{1/3}\text{Nb}_{2/3})\text{O}_3\text{-PbTiO}_3$ (PZN-PT), yield significantly higher electromechanical coupling coefficient than conventional polycrystalline ferroelectrics.¹ Thus far, superior piezoelectric properties have been demonstrated in bulk single crystal form. A major challenge is to prepare these materials as single crystal epitaxial films between epitaxial metallic oxide electrodes, and integrate them into microelectromechanical systems. This would allow these superior properties to be utilized with all the advantages of uniformity, low surface roughness, multilayer stacking, and performance associated with microelectronics based on the technology of thick film single crystal ferroelectrics.

Growth of epitaxial PMN-PT films with good electromechanical properties is known to be difficult due to the relatively poor thermodynamic stability of the perovskite phase relative to the pyrochlore phase and due to compositional complexity.²⁻⁴ It is also known that it is difficult to control the stoichiometry in this system due to Pb loss during film growth. Nonetheless, high quality epitaxial PMN-PT thin films have been grown by pulsed laser deposition^{2,3} and metalorganic chemical vapor deposition,⁴ among other methods.⁴ Typically, piezoelectric coefficients from 50 to 350 pC/N and relative dielectric constants between 300 and 2000 have been reported at room temperature.^{3,5} These val-

ues are lower than those of bulk single crystals, which is attributed to strain, substrate constraint, phase purity, and stoichiometry.

In this letter, we report the growth of high quality epitaxial PMN-PT thin films with stoichiometric composition by deposition onto miscut (001) SrTiO_3 substrates. Miscut substrates have been used to grow various high quality perovskite oxide thin films, such as $\text{La}_{2-x}\text{Sr}_x\text{Cu}_2\text{O}_4$,⁶ $\text{Ba}_2\text{Sr}_2\text{Ca}_{n-1}\text{Cu}_n\text{O}_{20+4}$,⁷ $\text{YBa}_2\text{Cu}_3\text{O}_{7-\delta}$,⁸ and $\text{Sr}_{1-x}\text{Ca}_x\text{RuO}_3$ ($0 \leq x \leq 1$).^{9,10} It is generally believed that the miscut substrate changes the growth mechanisms of thin films, which leads to corresponding changes in their electrical transport and magnetic behavior.

90° off-axis magnetron sputtering has been attractive and widely used for large area deposition of high quality complex oxide thin films because of its simplicity and reproducibility.¹¹ It has already been demonstrated that this process can grow various perovskite oxide epitaxial ferroelectric heterostructures, such as $\text{SrRuO}_3/\text{PZT}/\text{SrRuO}_3$, with the smooth surfaces required for multilayered device applications.¹¹

The sputtering atmosphere consisted of 120 mTorr Ar and 80 mTorr O_2 . The substrate block temperature was held at 600°C . The miscut of the SrTiO_3 (STO) substrates was varied from 0° to 8° away from the (001) face toward [001]. Results reported here are for PMN-PT films 1300 and 5200 Å thick.

For electrical characterization we have also grown

^{a)}Electronic mail: eom@engr.wisc.edu

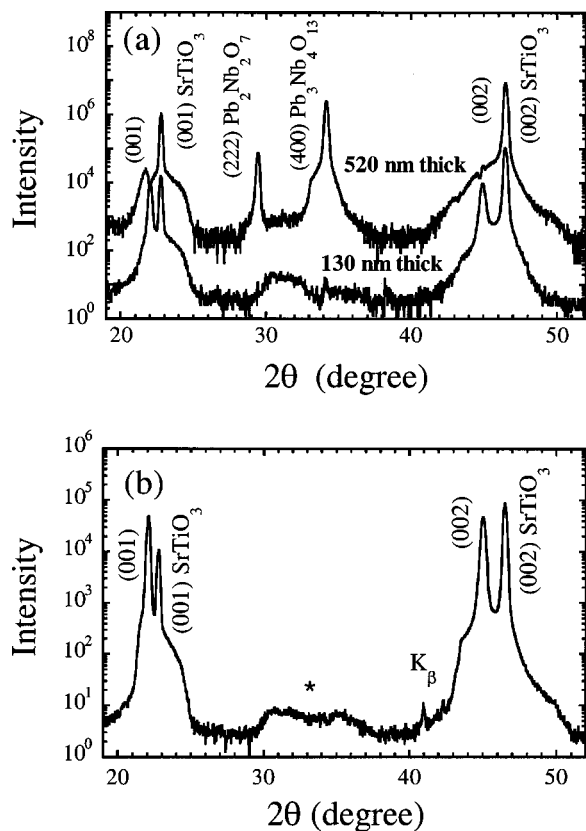


FIG. 1. X-ray diffraction θ - 2θ scans of PMN-PT films (a) 1300 and 5200 Å thick grown on exact (001) SrTiO₃ substrates and (b) 5200 Å thick grown on 8° miscut substrate. The broad peak between 29° and 38° with very low intensity below 10 from (001) SrTiO₃ substrate is labeled by (*).

PMN-PT on epitaxial SrRuO₃ (SRO) bottom electrodes. X-ray diffraction shows that all the SRO films deposited on (001) STO substrates (both exact and vicinal) had a purely (110) texture normal to the substrate. The surface of SRO is extremely smooth, which is important for multilayered device fabrication. The microstructure and orientation domain configurations of SRO films grown on both exact and miscut (001) STO substrates were studied in details in previous works.^{12,13}

Phase purity was found to be strongly dependent on both film thickness and miscut angle. Relatively thin films (1300 Å) on exact (001) STO substrates show only the perovskite phase in x-ray diffraction spectra. However, thick films (5200 Å) are found to have large amounts of second phases, as shown in Fig. 1(a). The second phase peaks in x-ray diffraction are identified as the (222) reflection of rhombohedral pyrochlore Pb₂Nb₂O₇ and the (400) reflection of cubic pyrochlore Pb₃Nb₄O₁₃, respectively.^{2,14} In contrast, 5200 Å thick films deposited on 8° miscut substrates display strong perovskite PMN-PT peaks, as shown in Fig. 1(b). Such a dramatic difference in x-ray diffraction patterns suggest that the miscut provides a mechanism promoting single crystal epitaxial growth. The measured full width at half maximum (FWHM) of the rocking curve for the PMN-PT (002) reflection is 0.41°, which is close to the value (0.32°) of a 0.65PMN-0.35PT bulk single crystal.¹⁵ The relatively broad rocking curve for PMN-PT may be explained by the existence near the morphotropic phase boundary of a mixture of two PMN-PT phases with rhombohedral and tetragonal

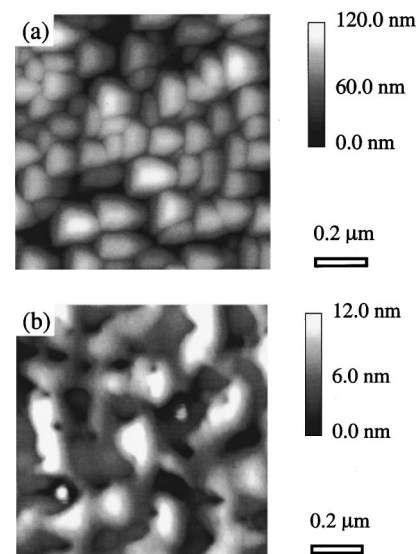


FIG. 2. AFM images of PMN-PT films grown on (001) SrTiO₃ substrates with (a) 0.8° and (b) 8° miscut angles.

structures.¹⁶ The off-axis azimuthal ϕ scan for the PMN-PT (101) reflection shows cube on cube in-plane epitaxial arrangement on (001) STO substrate.

The composition of the films has been determined by wavelength dispersive x-ray fluorescence spectroscopy (WDS). The composition for the film on the 8° miscut substrate shows a slight deficiency of Pb ($-4.7 \pm 0.9\%$), which can be compared with the value $-2.5 \pm 0.9\%$ for 0.73PMN-0.27PT single crystals used as a standard sample.¹⁵ The film on the 0° miscut substrate shows a large deficiency of Pb ($-15.3 \pm 0.8\%$), even though the film was deposited under identical conditions, and in the same deposition run.

The effects of miscut on surface morphology of these PMN-PT films have been investigated by atomic force microscopy (AFM). The surface of the film grown on the 8° miscut substrate is quite different from that of the film on the 0.8° miscut substrate, as shown in Fig. 2. The film on the 8° miscut substrate is extremely smooth with a root mean square (rms) roughness of 2 nm over a $5 \mu\text{m} \times 5 \mu\text{m}$ scan area, whereas the rms roughness of the film on 0° miscut angle is 21 nm. The granular shape present for the 0.8° miscut sample disappears for the larger miscut angle.

Further study on microstructure of these PMN-PT films has been done by transmission electron microscopy (TEM), including selected area electron diffraction (SAED). Figures 3(a) and 3(b) are cross-sectional TEM images of two 5200 Å thick films grown on 0.8° and 8° miscut substrates, respectively. For films on 0.8° miscut substrates, near the film/substrate interface the pure perovskite phase of PMN-PT grows, but the pyrochlore phases nucleate on top of the perovskite phase and the volume fractions of the pyrochlore phases increase with film thickness. These results are consistent with the x-ray diffraction data. The film on the 8° miscut substrate consists of the perovskite phase with only a small volume fraction of structure embedded in the perovskite, as indicated by arrows in Fig. 3(b). The pyrochlore phase with a shape of longish stick cut in pieces, so the pyrochlore phase is isolated. The inset on the left-hand side of Fig. 3(b) shows a SAED pattern which corresponds to the [010] zone elec-

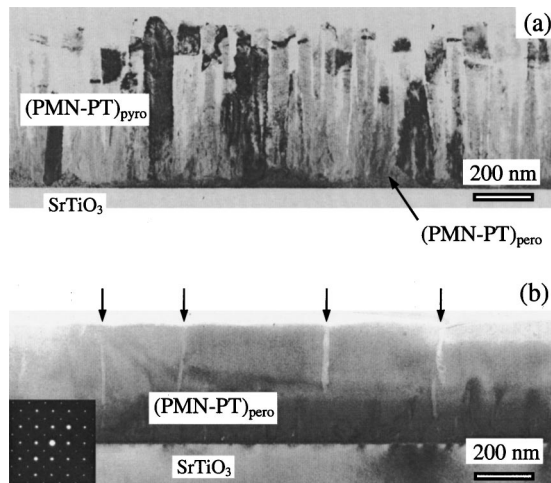


FIG. 3. Cross-sectional bright field TEM images of PMN-PT films grown on (001) SrTiO₃ substrates with (a) 0.8° and (b) 8° miscut angles. The inset is the selected area electron diffraction pattern.

tron diffraction pattern of PMN-PT. These results further confirm that epitaxial PMN-PT with good crystalline quality can be grown on (001) STO substrates with an 8° miscut angle.

The relative dielectric constant of the film on the 8° miscut substrate is 1000 under a small signal oscillation voltage of 0.2 kV/cm, whereas the film on 0° miscut substrate shows a very small dielectric constant of 80. The 8° miscut sample shows a polarization hysteresis loop with a large remnant polarization of 20 $\mu\text{C}/\text{cm}^2$ and a coercive field of 25 kV/cm at room temperature, as shown in Fig. 4(a). The temperature dependence of the dielectric constant illustrated in Fig. 4(b) show a relaxor behavior for this composition.¹⁶ The temperature of the maxima in the dielectric constant at 1000 Hz is about 145 °C, which is similar to the transition temperature (150 °C) for 0.70PMN–0.30PT single crystals.¹⁵

The miscut of the STO substrate plays an important role in the growth of films with stoichiometric composition, in a manner which we believe is related to terrace length variation with miscut angle.¹⁰ This in turn affects the stabilization of volatile Pb. Similar phenomena have been postulated for CaRuO₃ thin films containing volatile Ru.¹⁷

In summary, it has been demonstrated that, by employing miscut (001) STO substrates, epitaxial thin films of the relaxor ferroelectric PMN-PT can be grown with a near-stoichiometric composition. Films on 8° miscut substrates show relaxor behavior similar to that of single crystals. A large remnant polarization of 20 $\mu\text{C}/\text{cm}^2$ and a small coercive field of 25 kV/cm are obtained at room temperature. These films, with high crystalline quality and smooth surfaces, will allow us to grow high quality multilayer heterostructures of single crystal piezoelectric PMN-PT/SRO conductive oxides.

This work was supported by NSF Grant No. DMR-980244, DMR-9973801 to one of the authors (C.B.E.) and KOSEF through a Postdoctoral Fellowship to an author (S.D.B.). S.K.S. acknowledges support from the U.S. DOE Office of Science under Contract W-31-109-Eng-38.

¹S.-E. Park and T. R. ShROUT, J. Appl. Phys. **82**, 1804 (1997).

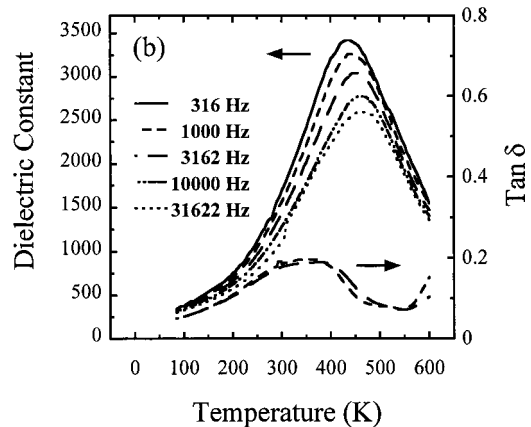
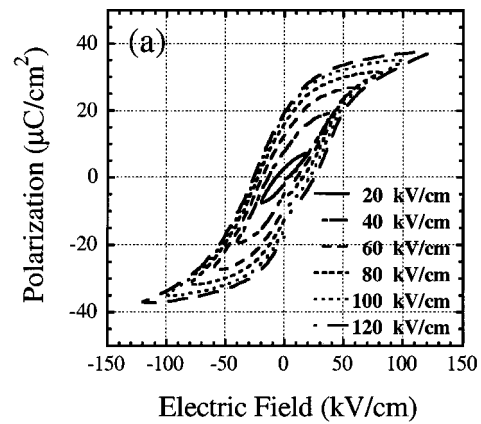


FIG. 4. Electrical properties of the PMN-PT film grown on (001) SrTiO₃ substrate with 8° miscut angle: (a) displacement hysteresis loop with applied voltages of 20, 40, 60, 80, 100, and 120 kV/cm, and (b) temperature dependence of permittivity and dielectric loss.

- ²D. Lavric, R. A. Rao, Q. Gan, J. J. Krajewski, and C. B. Eom, *Integr. Ferroelectr.* **21**, 499 (1998).
- ³J.-P. Maria, W. Hackenberger, and S. Trolier-McKinstry, *J. Appl. Phys.* **84**, 5147 (1998); J.-P. Maria, J. F. Shepard, Jr., S. Trolier-McKinstry, T. R. Watkins, and A. E. Payzant (unpublished).
- ⁴S. Stemmer, G. R. Bai, N. D. Browning, and S. K. Streiffer, *J. Appl. Phys.* **87**, 3526 (2000); G. R. Bai, S. K. Streiffer, P. K. Baumann, S. Stemmer, O. Auciello, K. Ghosh, A. Munkholm, C. Thompson, R. A. Rao, and C. B. Eom, *Appl. Phys. Lett.* **76**, 3106 (2000).
- ⁵V. Nagarajan, S. P. Alpay, C. S. Ganpule, B. K. Nagaraj, S. Aggarwal, E. D. Williams, A. L. Roytburd, and R. Ramesh, *Appl. Phys. Lett.* **77**, 438 (2000).
- ⁶J. Kwo, R. M. Fleming, H. L. Kao, D. J. Werder, and C. H. Chen, *Appl. Phys. Lett.* **60**, 1905 (1992).
- ⁷J. N. Eckstein, I. Bozovic, D. G. Schlom, and J. S. Harris, Jr., *Appl. Phys. Lett.* **57**, 1049 (1990).
- ⁸S. K. Streiffer, B. M. Lairson, and J. C. Bravman, *Appl. Phys. Lett.* **57**, 2501 (1990).
- ⁹C. B. Eom, R. J. Cava, R. M. Fleming, J. M. Phillips, R. B. Van Dover, J. H. Marshall, J. W. P. Hsu, J. J. Krajewski, and W. F. Peck, Jr., *Science* **258**, 1766 (1992).
- ¹⁰Q. Gan, R. A. Rao, and C. B. Eom, *Appl. Phys. Lett.* **70**, 1962 (1997).
- ¹¹C. B. Eom, R. B. Van Dover, J. M. Phillips, D. J. Werder, J. H. Marshall, C. H. Chen, R. J. Cava, R. M. Fleming, and D. K. Fork, *Appl. Phys. Lett.* **63**, 2570 (1993).
- ¹²J. C. Jiang, X. Pan, and C. L. Chen, *Appl. Phys. Lett.* **72**, 909 (1998).
- ¹³J. C. Jiang, X. Pan, W. Tian, Q. Gan, and C. B. Eom, *Appl. Phys. Lett.* **72**, 2963 (1998).
- ¹⁴S. L. Swartz and T. R. ShROUT, *Mater. Res. Bull.* **17**, 1245 (1982).
- ¹⁵S.-E. Park and T. R. ShROUT (unpublished).
- ¹⁶S. W. Choi, T. R. ShROUT, S. J. Jang, and A. S. Bhalla, *Mater. Lett.* **8**, 253 (1989).
- ¹⁷Q. Gan and C. B. Eom (unpublished).